Proceedings World Geothermal Congress 2000
Kyushu - Tohoku, Japan, May 28 - June 10, 2000

THE FAST-C SIMULATORS FOR DENSITY-DRIVEN FLOW
APPLICATION TO GEOTHERMAL MODELLING

Ekkehard Holzbecher
Institute of Freshwater Ecology and Inland Fisheries (IGB), Rudower Chaussee 30, 12489 Berlin, Germany

Key Words: FAST, modelling, density-driven flow, convection, porous medium, streamfunction, vorticity

ABSTRACT

The FAST-C software is designed to run models for density-driven flow in porous media and in free fluids. The codes are equipped with the GeoShell graphical user interface which allows user-friendly input, control and variation of all relevant parameters. The software has been applied to several problems in which density-driven flow patterns are involved: free and forced convection, oscillatory convection, saltwater intrusion, saltwater upconing, the saltdome problem and the salt-lake problem.
While the general code allows the set-up of three-dimensional models, there is a special version for two-dimensional modeling, FAST-C(2D), containing several advanced options.
As an application of FAST-C(2D) code a synthetic test-case of geothermal flow is modeled. The mixed convection regime in the example can be characterized by two non-dimensional numbers, the Rayleigh number and a new dimensionless number which relates buoyancy to external forces. The example demonstrates how numerical experiments in the space of dimensionless variables can be used to understand the complex interaction of various processes in a geothermal system.

1. INTRODUCTION

Density-driven flow is induced by temperature and/or salinity gradients. Flow and transport processes are coupled when there is influence of temperature or salinity on fluid density. The coupling complicates the situation in comparison to usual applications with constant density in which flow is not affected by transport processes.
When density differences in a system, either in porous media or in free space, are small, flow and heat transport can be modelled separately. But there are several situations in which the density coupling has to be taken into account. A small list may suffice here: thermal and saline convection, saltwater intrusion, saltwater upconing, interaction between salt-lakes and groundwater, contact with heating and cooling facilities, heat pumps. In geothermal phenomena density gradients are involved that are too big to be neglected.
Often the transition from one flow regime to another is characterized by a certain threshold - by density gradients or by a dimensionless number. A well-known example is Bénard convection for which there is a transition from conduction to stable convection at the critical Rayleigh number.

2. DIFFERENTIAL EQUATIONS

The FAST software is designed for the set-up of numerical models. There are several parts of the FAST package which can be used for different phenomena. FAST-A enables 3D-modeling of flow in saturated and unsaturated porous media (Holzbecher, 1996). FAST-B(2D) allows 2D-modeling of transport processes, including sorption, decay and degradation (Holzbecher, 1996). With FAST-C code coupled flow and transport models in 3D can be set-up. The FAST-C(2D) code is designed for modeling density-driven flow in 2D vertical cross-sections. As the latter is the most advanced part of the FAST package and especially suited for modeling geothermal phenomena, this contribution deals with FAST-C(2D) only. A textbook including software on CD-ROM was published by Holzbecher (1998a) recently. The book shows how the numerical techniques are derived from fundamental principles, describes details of the code and how to use it. Furthermore application and test-cases are described and modeled.
Using the FAST-C(2D) code the modeler can choose between several model options. Steady state modeling or transient simulations can be performed. The driving force for density-driven flow can be temperature or salinity gradients. The input parameters depend on the choice between dimensionless formulation and physical units. The most recent version lets the user choose between porous medium and free fluid flow.
The numerical code is derived from a set of partial differential equations. The differential equations themselves are a mathematical expression of fundamental principles like mass and energy conservation. Well established empirical relations are used to describe mass and energy fluxes: Darcy's Law, Fick's Law and Fourier's Law.
In dimensionless formulation thermal convection is described by the set of three differential equations:

$$\frac{\partial \theta}{\partial t} = \nabla^2 \theta - \frac{\partial \Psi}{\partial x}\frac{\partial \theta}{\partial z} + \frac{\partial \Psi}{\partial z}\frac{\partial \theta}{\partial x} \qquad (1)$$

$$\frac{1}{\mathrm{Pr}}\frac{\partial \omega}{\partial t} = \nabla^2 \omega - \frac{1}{\mathrm{Pr}}\left(\frac{\partial \Psi}{\partial x}\frac{\partial \omega}{\partial z} - \frac{\partial \Psi}{\partial z}\frac{\partial \omega}{\partial x}\right) - \mathrm{Ra}\cdot\frac{\partial \theta}{\partial x} \qquad (2)$$

$$\nabla^2 \Psi = -\omega \qquad (3)$$

with dimensionless streamfunction Ψ, vorticity ω and normalized temperature θ. In the porous medium case equation (2) can be replaced by an explicit formula for vorticity:

$$\omega = \pm \mathrm{Ra}\cdot\frac{\partial \theta}{\partial x} \qquad (4)$$

All relevant physical parameters are combined in dimensionless numbers - the Rayleigh-number

$$\mathrm{Ra} = \frac{k \cdot \gamma \cdot g \cdot \Delta\rho \cdot H}{\mu \cdot D} \quad (5)$$

and the Prandtl-number:

$$\mathrm{Pr} = \frac{\mu}{D \cdot \rho} \quad (6)$$

with permeability k, ratio of heat capacities γ, acceleration due to gravity g, reference density ρ, maximum density difference $\Delta\rho$, system height H, dynamic viscosity μ, and thermal diffusivity D. For free fluids the permeability k has to be replaced by H^2 and γ by 1:

$$\mathrm{Ra} = \frac{g \cdot \Delta\rho \cdot H^3}{\mu \cdot D} \quad (7)$$

In the porous medium the Rayleigh number is the single dimensionless parameter.
For the porous medium case Holzbecher (1998a) shows in detail how differential equations are derived from basic principles. Additionally the details of transformation into dimensionless form is given there.

3. NUMERICAL APPROACH

The differential equations are discretized using a standard finite difference (FD) approach. The user has influence only on the FD representation of the 1st order terms - an option that can be important because it allows control of numerical dispersion. In transient simulations the modeler has the choice of timestepping procedures.
For each differential equation a linear system of equations results. In a Picard type of solution algorithm these linear sets are solved successively until a certain criterion is fulfilled. The criterion can be altered by the user specifying a maximum number of iterations and tolerance.
Linear systems are solved using conjugate gradient (CG) methods, with or without preconditioning. Different CG variants are used depending on the type of linear systems - symmetric or unsymmetric matrices are treated differently. The user has some additional options to alter predefined CG-parameters.
The code is equipped with a graphical user interface (GeoShell) for PCs. The interface comes with standard techniques like a menu bar with submenu entries, with input boxes, alert messages and other tools (see Figure 1). The menu automatically adjusts to the selected model type: necessary parameters are enabled, unnecessary parameters are disabled. Clicking buttons and entering values in input boxes makes work easy for the modeler. The shell software provides a graphical representation of the model area giving the user an easy way to input change and control input data. This is extremely useful when input data are distributed. Moreover a large online help library provides information that can be useful not only for the novice but for advanced users also.
There are several options for the boundary conditions too. For streamfunction and temperature Dirichlet and Neumann type conditions can be specified. Boundary conditions can be different from one part of the boundary to the other. Using this option various examples of density-driven flow can be set-up and modeled. As an example a schematic view of boundary conditions for modeling free convection - the classical Bénard example in a vertical cross-section - is given in Figure 2.

4. APPLICATIONS AND TEST CASES

Several examples have been calculated using the FAST-C(2D) code - for testing purposes and for application cases. The Henry problem has become a classical testcase for saltwater intrusion modeling (Holzbecher 1998a). The Nile-delta aquifer in Egypt was treated as an application case for seawater intrusion (Holzbecher and Baumann, 1994). A saltwater upconing example was published by Holzbecher (1995) and Holzbecher and Heinl (1995). Holzbecher (1998b) examined the change of convective flow patterns when variations of viscosity are considered. In a similar expertise the influence of nonlinear density dependency was studied (Holzbecher, 1997). Recently the modeling of ground- and surface water in the vicinity of salt-lakes has drawn some attention (Holzbecher 1999a, b). Several other examples, like the Elder problem and oscillatory convective motions can be found in the above mentioned textbook (Holzbecher 1998a).

5. GEOTHERMAL TESTCASE

5.1 Conceptual Model

For codes designed to set-up geothermal models a test case was proposed by Yusa (1983). The intention of the hypothetical example is to estimate the relative importance of potential flow and thermal convective flow.
A vertical cross-section of an aquifer is studied in which the flow pattern is influenced from above and below. At the bottom the subsurface fluid is in contact with a high temperature zone, from which heat - not fluid - enters the studied region. At the top there is a prescribed potential flow. Seasonal changes that are characteristic for near-surface potential flow in field situations are neglected in order to keep the test-case simple. Input parameters for the test case are listed in Table 1.
The proposed example has been used by several researchers to test their codes. Yano (1989) tested a finite element code based on a slightly differing formulation of differential equations. With a former version of the FAST-C(2D) code Holzbecher and Yusa (1995) obtained very similar results than in the original publication (Yusa, 1983). Springer (see Holzbecher 1998a) tested his finite element THERMOD code, confirming basic features of geothermal flow found in former publications.

5.2 Numerical Model

A new numerical model is set up with FAST-C(2D). A schematic view of the test-case example in a vertical cross-section and the boundary conditions is given in figure 3. The system is closed for fluid at three boundaries. In the streamfunction formulation a constant value Ψ=0 is prescribed there. At the top boundary the Neumann condition specifies the horizontal velocity along the upper edge: $\partial\Psi/\partial z = v_{bound}$. Thus strength of potential flow enters the model via this Neumann type condition.
There is a high temperature boundary condition at the location of contact with the hot formation in the subsurface and a low

temperature boundary condition on the top boundary. On vertical boundaries there is no diffusive and advective heat flux.
The modeling in this paper is done with a fine grid of 200 equal blocks in the horizontal and 40 equal blocks in the vertical direction. Four cases are modeled differing only in the strength of the potential flow, i.e. the boundary condition at the upper boundary is changed. The four cases are distinguished by the hydraulic gradient at the top edge, which is zero in the first simulation, 1%, 3% and 5% in the following model runs. All transient simulations start with the constant (low) temperature situation. Simulated time-period is the same for all different: 0.78 dimensionless time units.

5.3 FAST-C(2D) Results

Results of the model are shown in Figure 4. For all four cases two figures are shown, one showing the contours of the streamfunction, the other the temperature distribution. Thus figures 4a, 4c, 4e and 4g show streamfunction contours at the end of the simulated time period for the four different cases. Contour levels are chosen equidistantly, not only within one figure but also from one figure to the other. Only in figure 4a the spacing between contours is reduced one order of magnitude because otherwise the flow pattern would not be visible any more. Figures 4b, 4d, 4f and 4h show temperature distribution in equal steps between T_{min} and T_{max} at the end of the simulated time period.
The cases for potential gradients 0, 1% and 5%, represented by figures 4a-4d and 4g-4h, seem to be quasi-steady state. Only marginal changes are observable from one time step to the other. There is a transient development captured in figures 4e and 4f for the case with 3% potential.
Altogether the figures confirm the findings from former calculations for Yusa's test-case, although in detail there are quite big differences, even when the new results with FAST-C(2D) are compared with output obtained on a coarser grid. Relatively narrow tongues of hot fluid moving upward along the vertical boundary adjacent to the heat source, which were found in coarse grid simulations, are not be confirmed by the fine grid results.
Generally solutions of differential equations are approximated better by numerical models with finer discretization. Thus it is not unusual that a coarse grid simulation fails to give some features of the real solution. Similar observations have been made and discussed for the Elder example (Holzbecher 1998a).

5.4 Epilogue

A new dimensionless parameter Co can be introduced to describe the balance between potential and thermal convective flow in the geothermal test-case. Holzbecher and Yusa (1995) propose the definition:

$$\mathrm{Co} = \frac{g \cdot \Delta\rho}{\partial p / \partial x\big|_{top}} = \frac{k \cdot g \cdot \Delta\rho}{\mu \cdot v_{bound}} \qquad (8)$$

where v_{bound} is the velocity prescribed at the top boundary. With increasing number Co thermal convection becomes more important. With decreasing Co the relative importance of potential flow rises.
A classification of flow patterns using the dimensionless number Co is given in Table 2. For small values of Co convective motions can not be recognized. For high values of Co (for v_{bound}=0) there is one convection roll. In the transition zone between these two regimes two convection rolls can be observed and there is a flow field with thermal transients ejected from the high temperature region.
The new Co-number in the second form of equation (8) turns out to be useful in other applications of mixed convection as well. The new dimensionless number can be used in all cases in which a second moment, besides buoyancy, determines the pattern of fluid motions in the considered system. Often a characteristic velocity is explicitly or implicitly given, describing the additional outer moment, which can be used in the definition of Co in equation (8).
The Henry problem for saltwater intrusion can be recognized as such a problem. In a series of numerical experiments Holzbecher (1998a) shows that it is convenient to use Co to estimate of the intrusion (penetration) length of the salt-water front.
Holzbecher (1999b) explains rigorously how Co can be used to classify mixed convection processes below a saline disposal basin. Another test-case in which Co has been introduced successfully is the salt-dome problem (Holzbecher, 1998a).
Altogether it can be concluded that numerical experiments with dimensionless parameters are a useful tool for describing complex flow systems. The FAST-C(2D) code is a powerful and user-friendly tool to perform such experiments, although it is applicable for formulations with physical units as well.

REFERENCES:

- Holzbecher, E. (1995), Modeling of saltwater upconing, in: Wang S. (Ed.) *II. Int. Conf. Hydro-Science and Hydro-Engin.*, Proceedings, Vol. 2, Beijing, 858-865.
- Holzbecher, E., Heinl, M. (1995). Anisotropy and dispersivity effects on saltwater upconing, in: Abousleiman, Y., Brebbia, C.A., Cheng, A.H.-D., Quazar, D. (eds), *Comp. Methods and Water Ressources III*, Proc., Comp. Mech. Publ., Southampton, pp117-126.
- Holzbecher, E., (1996). *Modellierung dynamischer Prozesse in der Hydrologie: Grundwasser und ungesättigte Zone*, Springer Publ., Heidelberg.
- Holzbecher, E. (1997). Numerical studies on thermal convection in cold groundwater, *Intern. Journal of Heat and Mass Transfer*, Vol. 40 (3), pp.605-612.
- Holzbecher, E. (1998a). *Modeling Density-Driven Flow in Porous Media*, Springer Publ., Heidelberg / New York. 286pp.
- Holzbecher, E. (1998b). The influence of variable viscosity on thermal convection in porous media, in: Nowak, A.J., Brebbia, C.A., Bialoki, R., Zerroukat, M. (eds), Heat Transfer 98, Proc., Comp. Mech. Publ., Southampton, pp115-124.
- Holzbecher E. (1999a). Salinization of Groundwater from Salt Lakes - Conceptual and Numerical models, *Int. Conf. LAKE99*, Copenhagen, Vol. I, Contribution S4-B2.
- Holzbecher E. (1999b). Comment on 'Mixed convection processes below a saline disposal basin' by Simmons C.T. and Narayan K.A. (Journal of Hydrology Vol. 194 (1997) 263-285), submitted to: Journal of Hydrology
- Holzbecher, E., Baumann R., (1994). Numerical simulations of saltwater intrusion into the Nile Delta Aquifer, in: Peters, A., Wittum, G., Herrling, B., Meissner, U., Brebbia, C.A, Gray, W.G., Pinder, G.F., (eds) *Comp. Meth. in Water Res. X*, Proc. Vol.2, Kluwer Publ., Dordrecht, pp1011-1018.

- Holzbecher, E., Yusa, Y., (1995). Numerical Experiments on Free and Forced Convection. *Intern. Journal of Heat and Mass Transfer*, Vol. 38 (11), pp.2109-2115.
- Yano, Y. (1989). A practical procedure for vertical two-dimensional hydrothermal simulation by finite element method, *J. Jap. Assoc. Petrol. Eng*., Vol. 54, pp18-31.
- Yusa, Y. (1983). Numerical experiment of groundwater motion under geothermal condition - vying between potential flow and thermal convective flow, *J. of the Geothermal Res. Soc. of Japan*, Vol. 5(1), pp23-38.

Tables

Symbol	Parameter	Value
T_{min}	minimum temperature	20°C
T_{max}	maximum temperature	250°C
H	height	1000 m
L	length	5000 m
$\Delta\rho$	density difference	230 kg/m^3
μ	dynamic viscosity	2. 10^{-4}kg/m/s^2
k	permeability	10^{-14} m^2
D	thermal diffusivity	10^{-6} m^2/s
γ	ratio of heat capacities	2
Ra	Rayleigh number	113
$\partial h/\partial x\|_{top}$	hydraulic gradient	0, 1%, 3%, 5%

Table 1: Input parameters for geothermal test case

Hydraulic gradient	*Co=Ra/Pe*	Flow pattern
0.0	∞	one steady roll
1 %	23.06	two steady convection rolls
3 %	7.69	no steady state
5 %	4.69	no convection

Table 2: Flow pattern classification for geothermal test case

Figures

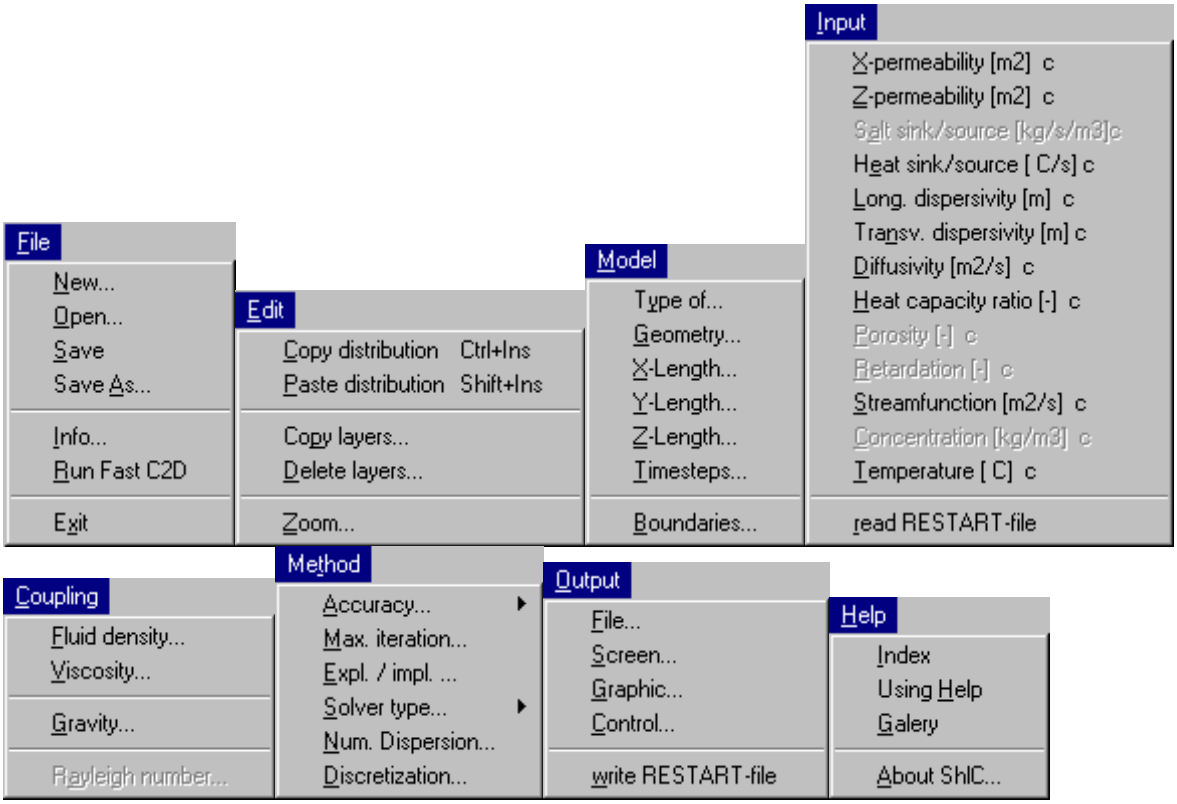

Figure 1: Main menu and submenu entries of GeoShell user interface

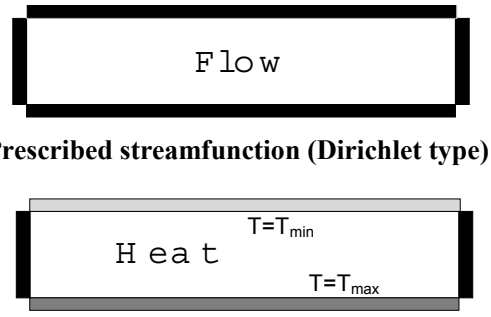

Figure 2: Schematic view of free convection test case

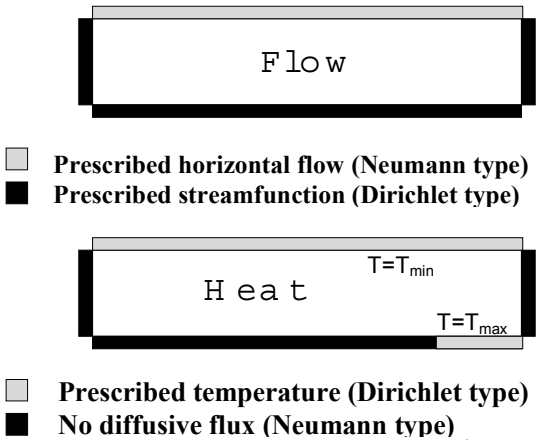

Figure 3: Schematic view of geothermal testcase

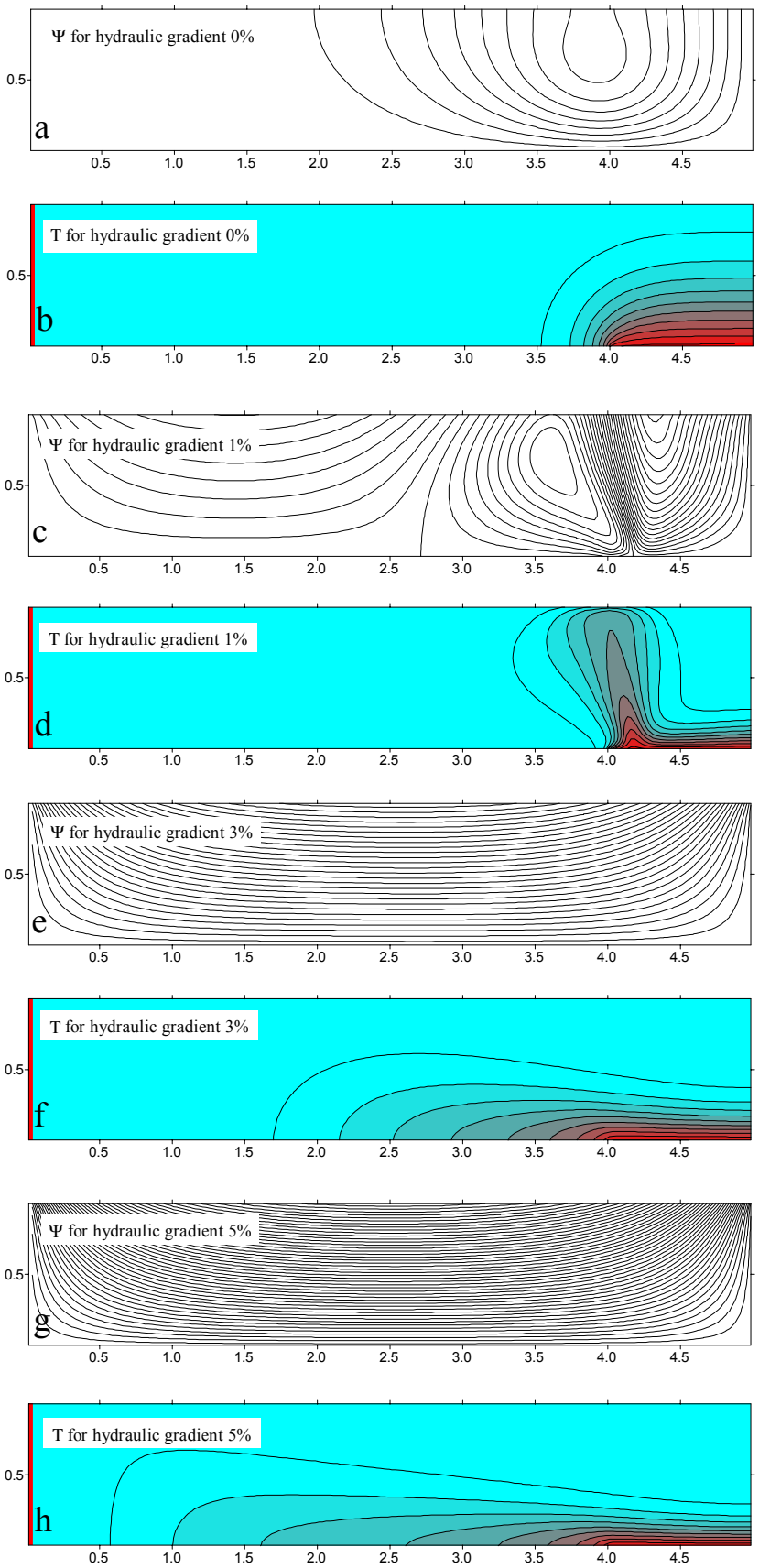

Figure 4: FAST-C(2D) results for the geothermal test case with refined grid (see text for further explanation)